

VERTEX-BASED NETWORKS TO ACCELERATE PATH PLANNING ALGORITHMS

Yuanhang Zhang Jundong Liu

School of Electrical Engineering and Computer Science
Ohio University

ABSTRACT

Path planning plays a crucial role in various autonomy applications, and RRT* is one of the leading solutions in this field. In this paper, we propose the utilization of vertex-based networks to enhance the sampling process of RRT*, leading to more efficient path planning.

Our approach focuses on critical vertices along the optimal paths, which provide essential yet sparser abstractions of the paths. We employ focal loss to address the associated data imbalance issue, and explore different masking configurations to determine practical tradeoffs in system performance. Through experiments conducted on randomly generated floor maps, our solutions demonstrate significant speed improvements, achieving over a 400% enhancement compared to the baseline model.

Index Terms— Path Planning, RRT*, Vertex, FCN

1. INTRODUCTION

Path planning aims to determine a feasible route for an autonomous agent to travel from a starting point to a target location within an environment while avoiding obstacles. This process has a wide range of applications across various domains. The common goal of path planning is to discover a route that is safe, efficient, and smooth.

Traditional path planning algorithms can be grouped into two primary categories: grid search-based and sampling-based. Among grid-search algorithms, the A* algorithm [1] is one of the most prominent solutions, capable of guaranteeing the finding of an optimal path if one exists; however, it may encounter difficulties in high-dimensional state spaces. Sampling-based algorithms, such as *Rapid Random-exploring Trees* (RRT) [2] and *Optimal Rapid Random-exploring Trees* (RRT*) [3], operate through randomly selecting states from the state space, rather than investigating all possible states, therefore speeding up the exploration process. RRT uniformly sample states within the state space while gradually building a tree structure of these states. RRT* enhances RRT by reorganizing the tree, granting it probabilistic completeness and asymptotic optimality.

Recently, machine learning-based approaches have been proposed to address the intricate challenges associated with path planning. These approaches can generally be categorized into supervised learning (SL) and reinforcement learning (RL) methods. SL-based solutions perform perception and decision-making simultaneously, predicting control policies directly from raw input images [4]. RL-based methods, on the other hand, rely on human-designed reward functions, allowing learning agents to explore policies through trial and error [5]. While promising, learning-based path planning solutions often lack theoretical guarantees on performance. Moreover, SL requires annotated data, which can be difficult or expensive to acquire.

The latest RRT-based solutions, including informed RRT* [6] and connect RRT [7], while using traditional strategies, are regarded as the state-of-the-art solutions in the field. This can be attributed to their flexibility in handling changes in the environment and their capability of to navigate high-dimensional state spaces. Moreover, RRT* has the guarantee of asymptotic optimality and probabilistic completeness, which ensures that the solution achieves optimality under specific conditions.

However, RRT* solutions suffer sensitivity to the initial solution and slow convergence to the optimal solution. To overcome these limitations, several network-based solutions have been proposed to speed up the sampling process. Trained on optimal paths, Neural RRT* [8] and Motion Planning Networks [9] predict the probability distribution of the path to achieving faster samplings. Neural Informed RRT* [10] guides RRT* tree expansion using an offline-trained neural network during online planning.

Although considerable speed-ups have been demonstrated in comparison to the original RRT* algorithm, the aforementioned acceleration networks commonly take the entire A* search space as the target area and estimate probabilities based on the proximity to optimal paths. Moreover, they may struggle with highly dynamic environments or those with rapidly changing obstacles, as the planning may become quickly outdated.

Thanks to Ohio University Research Committee (OURC) for funding.

In this paper, we propose to enhance the speed-up of the sampling process by shifting the target areas from the neighborhood of optimal paths to that of vertices (corners or turning points). Our design is based on the rationale that critical vertex points in the optimal paths provide an insightful and adequate abstraction of the paths, while requiring much less space. Focusing on vertices, however, results in a side effect that the training data would be highly imbalanced. We address this issue using focal loss [11] in this work. We also explore different thresholding setups for the network outputs to examine the system tradeoffs in performance.

2. BACKGROUND

Rapidly-Exploring Random Trees (RRTs) comprise a family of path planning algorithms that depend on incremental sampling. The RRT algorithm [2] starts with a single-vertex tree that represents the initial state and has no edges. Over each iteration, the algorithm generates a state x_{rand} from a uniform sampling of the search space and tries to link it to the nearest vertex x_{nearest} in the tree. If this linkage is feasible, the Steering function manipulates x_{rand} to produce x_{new} . The new state x_{new} and new edge $(x_{\text{nearest}}, x_{\text{new}})$ are then added to the growing tree.

The RRT* algorithm [3] introduces two additional procedures: $\text{Extend}(G, x_{\text{new}})$ function and the $\text{Rewire}(G)$ process. During the Extend procedure, RRT* searches for optimal parent vertices around x_{new} within a certain radius. After integrating x_{new} into the tree, RRT* rewires neighbor vertices to assess whether a path through x_{new} can provide a lower cost than the current path. The procedure of the RRT* algorithm is illustrated in Algorithm 1. $\text{ObstacleFree}(x_{\text{nearest}}, x_{\text{new}})$ function determines if the line segment connecting x_{nearest} and x_{new} is obstacle-free. RRT* is asymptotically optimal, which means that as the sampling iterations approach infinity, the path converges to the optimal path.

Algorithm 1: RRT*

Input: $x_{\text{init}}, x_{\text{goal}}, \text{Map}$

Output: $G = (V, E)$

```

1  $V \leftarrow \{x_{\text{init}}\}; E \leftarrow \emptyset;$ 
2 for  $i = 1, \dots, n$  do
3    $x_{\text{rand}} \leftarrow \text{UniformSample}();$ 
4    $x_{\text{nearest}} \leftarrow \text{Nearest}(G = (V, E), x_{\text{rand}});$ 
5    $x_{\text{new}} \leftarrow \text{Steer}(x_{\text{nearest}}, x_{\text{rand}});$ 
6   if  $\text{ObstacleFree}(x_{\text{nearest}}, x_{\text{new}})$  then
7      $\text{Extend}(G, x_{\text{new}});$ 
8      $\text{Rewire}(G);$ 
9 return  $G = (V, E);$ 

```

The Neural RRT* algorithm [8] trains a CNN model on successful path planning cases to generate a nonuniform sampling distribution. For a given task, the trained network can

predict the probability distribution of the optimal path for on the map, which can guide and speed up the sampling process.

3. METHOD

In this work, we propose a method to improve the Neural RRT* category by redirecting the sampling guidance from the neighborhoods of optimal paths to key vertices. To achieve this, we train a neural network called *VertexNet*, and subsequently integrate it with the RRT* algorithm.

3.1. VertexNet

Our VertexNet is designed to predict the likelihood of each pixel being a vertex on the optimal path, which we refer to as *vertex-ness*. We approach this task as an image mapping problem and address it using a fully convolutional network, as depicted in Fig. 1. The input to VertexNet consists of an RGB image representing a floor map, where obstacles, source, and target points are differentiated by distinct colors. The ground-truth is a corresponding vertex map extracted from the A* optimal path. The output of VertexNet is a vertex-ness map, which will subsequently be integrated into the RRT* algorithm to guide the sampling process.

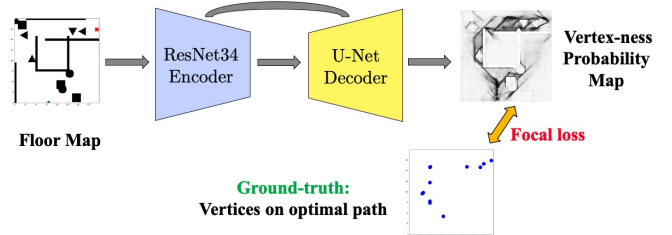


Fig. 1. Illustration of the proposed VertexNet. Best view on screen.

VertexNet is modified from the U-Net [12], primarily by adopting ResNet34, a residual network [13] as the backbone for the encoder. This modification aims to enhance the network’s ability to capture important features from the input images and facilitate effective training. The updated encoder consists of basic blocks as described in [13], each of which contains two 2-dimensional convolutional layers, two batch normalization layers, and one Rectified Linear Unit (ReLU) activation. In total, our network has 54 weighted layers and 41,221,168 parameters, among which, 19,953,520 are trainable. The network takes floor map images of size 200×200 as inputs.

3.1.1. Ground Truth and Training Objective

The ground-truth images in our work are generated following a three-step process. In the first step, we employ the A* algorithm to determine the optimal path for a floor map. Next, we

extract a number of vertex points on the optimal path based their vertex-ness (being corners or turning points). Finally, we create the ground-truth images by setting the pixels of the selected vertices to 0s, while the remaining pixels are set to 1s.

Vertices are chosen among the pixels on the path based on specific criteria. Specifically, only the end-points of line segments are considered as vertices, while intermediate points are excluded. Since the paths are generated within discrete image domains, the identification of straight lines becomes crucial. Straight lines can consist of line segments with consistent directions, as in Fig. 2(a). The red dash-lines in Fig. 2(b) could also be straight under a continuous domain, as their directions are not changed. Fig. 2(c) shows a similar case where we look ahead for three steps. It should be noted that the points x_i in all three cases should not be classified as turning points.

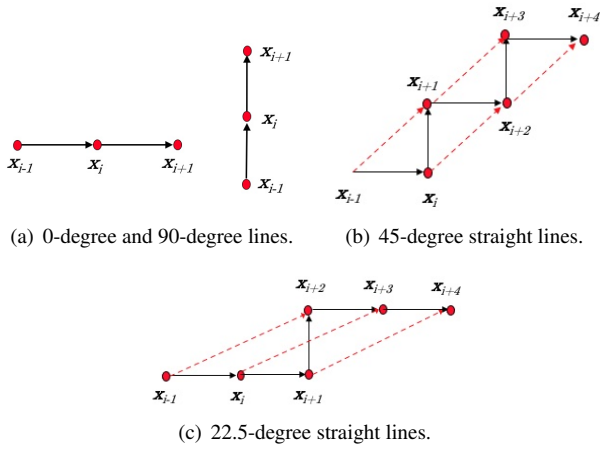


Fig. 2. Three cases of straight lines within the pixel domain.

Let $X_{\text{path}} = \{x_0, x_1, \dots, x_T\}$ be a path going through a sequence of positions within an image domain. To determine whether a point $x \in X_{\text{path}}$ should be considered as a turning point, we examine if there is a change in direction for any of the three step sizes in Fig. 2. In essence, we define a vertex as follows:

$$X_{\text{vertex}} = \{x \in X_{\text{path}} \mid \Delta(x_i - x_{i-1}) \wedge \Delta(x_i - x_{i-2}) \wedge \Delta(x_i - x_{i-3})\}$$

where Δ denotes the presence of a change in direction with a certain step size.

3.1.2. Loss Function

As very few pixels in each ground-truth image are selected as vertices, the ground-truth images tend to be predominately blank as vast majority (over 99%) of the pixels have intensity of 1s. This intensity imbalance would create a challenge for

image mapping problems. To tackle this issue, we adopt the focal loss [11] as the objective function for our VertexNet.

$$\text{FL}(p_t) = -(1 - p_t)^\gamma \log(p_t)$$

Compared to the cross-entropy loss, the focal loss adds a modulating factor $(1 - p_t)^\gamma$. This factor assigns varying weights to samples based on their difficulty of classification. Easy samples, which are more likely to be correctly classified, receive reduced weights, while harder samples are assigned higher weights. In our dataset, as the non-vertex pixels constitute the majority, they are categorized as easy samples, resulting in reduced contributions through the modulating factor. The focusing hyperparameter γ is adjustable, and based on empirical observations, we set it to 2 in our experiments.

3.2. VertexNet RRT*

After VertexNet is trained, it is integrated into the RRT* algorithm to enhance the sampling process. The integration process follows a similar design to that of Neural RRT* [8]. Taking a floor map as the input, the non-uniform sampler generated by VertexNet works together with the uniform sampler from RRT* to make informed sampling decisions. VertexNet plays a crucial role by providing probabilistic guidance for selecting the next sampling point, thus improving the overall sampling efficiency. Meanwhile, the uniform sampler ensures that the integrated algorithm retains its original properties of probabilistic completeness and asymptotic optimality.

The resulting algorithm is referred to as VertexNet RRT*, as outlined in Algorithm 2. Each sampler is assigned a 50% probability of being invoked, which is determined by the Rand() function. The Nearest function, Extend, Rewire and Steer function are all the same as in the original RRT* algorithm.

Algorithm 2: VertexNet RRT*

Input: $x_{\text{init}}, x_{\text{goal}}, \text{Map}, \text{VertexNet}$
Output: $G = (V, E)$

- 1 $\mathcal{O} = \text{VertexNet}(\text{Map}, x_{\text{init}}, x_{\text{goal}})$;
- 2 $V \leftarrow \{x_{\text{init}}\}; E \leftarrow \emptyset$;
- 3 **for** $i = 1, \dots, n$ **do**
- 4 **if** $\text{Rand}() > 0.5$ **then**
- 5 $x_{\text{rand}} \leftarrow \text{VertexNetSample}(\mathcal{O})$;
- 6 **else**
- 7 $x_{\text{rand}} \leftarrow \text{UniformSample}()$;
- 8 $x_{\text{nearest}} \leftarrow \text{Nearest}(G = (V, E), x_{\text{rand}})$;
- 9 $x_{\text{new}} \leftarrow \text{Steer}(x_{\text{nearest}}, x_{\text{rand}})$;
- 10 **if** $\text{ObstacleFree}(x_{\text{nearest}}, x_{\text{new}})$ **then**
- 11 $\text{Extend}(G, x_{\text{new}})$;
- 12 $\text{Rewire}(G)$;
- 13 **return** $G = (V, E)$;

3.2.1. Masked VertexNet RRT*

To explore different configurations, we develop a masked version of the VertexNet RRT* algorithm. In this variant, a mask is applied to the sampling probability distribution generated by VertexNet. The mask functions by setting probabilities below a specific threshold value, denoted as τ , to zero. In the original VertexNet RRT* algorithm, even pixels with low probabilities have a chance of being chosen as vertex points. However, with the applied mask, probabilities below the threshold value are disregarded, leading a higher likelihood of sampling actual vertex points.

4. EXPERIMENTS

Data We generated a total of 10,000 maps for our experiments. Each map consists of 12 randomly chosen start points and 12 randomly chosen goal points, resulting in a dataset of 1,440,000 maps in total. Fig. 3 shows five maps with different levels of complexity. In our experiments, 70% of the maps were used for training, and 30% for testing.

To ensure the simulation of diverse map scenarios, our map generator randomly selects a variable number of obstacles, including shapes like triangles, circles, squares, bars, and U-shaped obstacles. The orientation of each obstacle is also chosen randomly. Each map has a dimension of 200x200 pixels, and integer values are assigned to each pixel based on their respective classes. Traversable space is denoted by 0, obstacles are represented by 1, start points are labeled as 2, and goal points are labeled as 3.

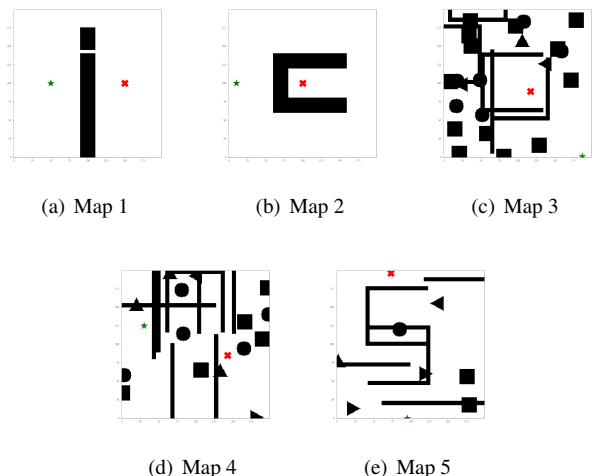


Fig. 3. Five floor maps with different complexities. In each map, green star denotes the start state and the red cross is the destination.

4.1. Sampling Probability Comparisons

The key design of our VertexNet RRT* lies in the modification of the training objective to focus on the turning points of the optimal paths. This modification is aimed to reduce the sampling space required for the RRT* algorithm. By comparing the resulting probability distribution predictions from models trained with distribution predictions from models trained with the vertex-based objective versus the path-based objective, we can assess the effectiveness of our approach.

Fig. 4 illustrates a representative example, where the optimal path and the extracted vertices are displayed in Fig. 4(a) and (b), respectively. Fig. 4(c) shows the probability distributions trained using the optimal paths in Neural RRT*, while Fig. 4(d) show the probability distributions trained using our VertexNet. As evident, the latter has much fewer bright areas, indicating that the sampling space of VertexNet RRT* is greatly reduced compared to the Neural RRT*.

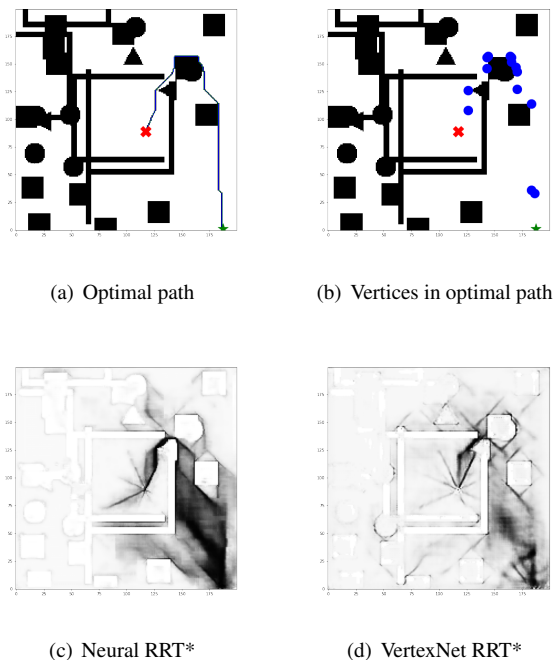


Fig. 4. Sampling distributions of Neural RRT* and VertexNet RRT*. Dark area depicts high probabilities, light area shows low probabilities. (a) Blue line is the optimal path. (b) Blue dots are the vertices in the optimal path. (c) Sampling probability distribution from Neural RRT*. (d) Sampling distribution from our VertexNet RRT*.

4.2. Path Planning Results and Analysis

We performed experiments on four different algorithms, namely RRT*, Neural RRT*, our VertexNet RRT* and

Table 1. Path Length comparisons of the *initial solutions*

	Map 1	Map 2	Map 3	Map 4	Map 5	Random Maps
RRT*	250.93±46.98	322.02±24.06	284.38±19.93	222.33±26.05	373.03±28.89	153.07±83.77
NRRT*	214.49±47.46	316.9±26.02	282.62±18.39	210.23±18.8	364.38±30.6	142.71±80.65
VNRRT*	215.85±47.96	312.17±23.2	283.94±18.57	212.53±19.55	361.57±30.98	145.75±81.38
M-VNRRT* $\tau=0.5$	164.18±35.44	304.33±23.00	293.17±21.17	205.7±17.52	351.48±32.01	134.25±79.92
M-VNRRT* $\tau=0.9$	154.02±24.01	313.67±25.77	296.76±22.96	202.30±16.42	344.03±29.34	133.98±80.73
M-VNRRT* $\tau=0.99$	163.62±32.51	302.72±23.08	306.46±29.52	198.09±18.85	346.61±24.52	136.55±82.49
Optimal	135.14	255.68	264.71	190.20	319.58	119.35

Optimal: Optimal path length

Table 2. Time Cost of finding *initial solutions*

	Map 1	Map 2	Map 3	Map 4	Map 5	Random Maps
RRT*	0.19±0.20	0.7±0.52	33.42±46.82	6.76±13.47	8.06±11.09	1.84±14.72
NRRT*	0.23±0.24	0.53±0.38	23.24±28.81	4.57±9.54	6.93±8.9	0.77±6.07
VNRRT*	0.18±0.19	0.64±0.44	11.15±14.83	2.29±3.57	5.69±7.23	0.45±2.17
M-VNRRT* $\tau=0.5$	0.15±0.17	0.62±0.43	5.56±5.83	1.20±1.63	6.22±8.36	0.85±5.09
M-VNRRT* $\tau=0.9$	0.10±0.08	0.76±0.53	5.22±6.82	1.83±2.49	8.81±11.89	0.62±3.60
M-VNRRT* $\tau=0.99$	0.20±0.19	0.88±0.83	10.36±32.27	3.56±4.77	4.58±4.38	1.44±12.27

Time cost to find the initial solution in seconds.

Table 3. Time Cost of finding *optimal solutions*

	Map 1	Map 2	Map 3	Map 4	Map 5	Random Maps
RRT*	1034.98±1055.17	50.97±35.56	47.20±57.36	28.55±17.03	36.19±23.21	29.62±102.66
NRRT*	36.48±37.57	16.45±8.27	35.28±30.45	9.62±10.92	19.63±14.10	19.38±62.62
VNRRT*	34.57±33.43	17.34±8.36	18.24±15.00	5.99±3.67	15.09±10.51	10.96±62.67
M-VNRRT* $\tau=0.5$	2.46±2.21	13.41±7.39	16.14±9.63	2.88±3.12	16.12±12.02	3.71±11.58
M-VNRRT* $\tau=0.9$	4.86±7.95	19.09±12.30	21.97±13.28	2.89±2.13	15.37±14.86	18.40±96.41
M-VNRRT* $\tau=0.99$	29.4±65.28	46.14±46.16	36.77±40.06	4.95±4.48	19.68±26.66	85.40±400.62

Time cost to find the optimal solution in seconds.

Masked VertexNet RRT*. We use the abbreviations RRT*, NRRT*, VNRRT* and M-VNRRT* in the upcoming presentation. The evaluations were conducted for both *initial solutions*, where each algorithm terminates upon reaching the destination, and *optimal solutions*, where each algorithm terminates after finding the optimal path.

We conducted experiments to find *initial solutions* on the five individual maps in Fig. 3, as well as 1,000 random maps selected from the test set. Each individual map underwent 1,000 trials for each algorithm to find an initial solution. The results for the random maps were averaged across the 1,000 maps. The performance of the algorithms was evaluated based on *Path Length* and *Time Cost*, as summarized in Table 1 and Table 2. Among the models, our VNRRT* algorithm demonstrated the fastest performance in finding the initial solution in the Random Maps settings, as indicated in Table 2. Moreover, the path length achieved by VNRRT* was comparable to that of the baseline Neural RRT*.

We further evaluated the performance of the algorithms in finding *optimal solutions*. Due to the time-consuming nature of finding optimal solutions, we reduced the number of experimental trials to 100. Among the algorithms tested, the M-VNRRT* $\tau=0.5$ algorithm consistently delivered the best results in experiments conducted on Map 1-4 and Random Maps. On the other hand, our VNRRT* algorithm achieved

the best performance on Map 5, as summarized in Table 3.

Fig 5 shows the speed improvements of the algorithms over RRT* on finding optimal solutions. Our VNRRT* outperformed NRRT* in almost all the experiments, except for Map 2, where its performance was 5% worse. However, the M-VNRRT* demonstrated relative improvements compared to NRRT* in all experiments, particularly in Map 3, Map 4, and Random Maps, where the improvements were 118.59%, 234.03%, and 422.37%, respectively.

As models' performance vary on individual maps, the Random Maps experiment provides a more objective evaluation by averaging results of 100 maps. The results are summarized in the rightmost column of Table 3. On average, the proposed VNRRT* algorithm shows an acceleration of 76.82% over the baseline NRRT* algorithm when converging to optimal paths. The M-VNRRT* with $\tau=0.5$ demonstrates an impressive improvement of 422.37% when compared to NRRT*.

In summary, our VNRRT* algorithm demonstrates a significant improvement of over 70% compared to NRRT* when converging to both the optimal and initial solutions. On the other hand, our M-VNRRT* $\tau=0.5$ exhibits superior performance in finding the optimal solution, being over 400% faster than NRRT*. However, it is 9.41% slower than NRRT* when finding initial solutions.

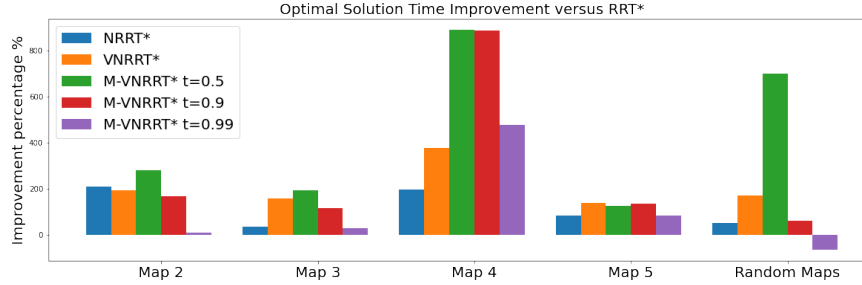


Fig. 5. Time improvements over RRT* on finding *optimal solutions*. Data are Maps 2-5 and Random Maps and the improvements are shown in percentage.

Our VNRRT* algorithm demonstrates superior speed in finding initial solutions (Table 2), possibly because it does not incorporate a mask that restricts the sampling points to optimal vertices. In contrast, the inclusion of a mask in the M-VNRRT* algorithm imposes more constraints on the sampling probability, therefore speed up convergence to the optimal solution. This is evident from the performance of M-VNRRT* $\tau=0.5$ in the optimal solution experiments (Table 3). Points with a probability prediction below 50% are less likely to be vertex points but still have a chance of being sampled. The masking process may have excluded these points, resulting in faster convergence to the optimal solutions.

5. CONCLUSION

In this work, we present a novel approach to improve the learned heuristic for path planning algorithms. Rather than using the entire optimal path line segment as the objective, we focus solely on the turning points of the optimal paths in our proposed VertexNet. This modification significantly enhances the speed of the path planning algorithms. We also introduce a mask to the sampler of VertexNet RRT*, which boosts the sampling probability of the actual vertices in the optimal path. This further accelerates the convergence speed to the optimal path. Overall, our approach provides a more efficient method for learning heuristics, which is important for future machine learning applications in path planning problems.

6. REFERENCES

- [1] Peter E Hart, Nils J Nilsson, and Bertram Raphael, “A formal basis for the heuristic determination of minimum cost paths,” *IEEE transactions on Systems Science and Cybernetics*, vol. 4, no. 2, pp. 100–107, 1968.
- [2] Steven M LaValle et al., “Rapidly-exploring random trees: A new tool for path planning,” 1998.
- [3] Sertac Karaman and Emilio Frazzoli, “Sampling-based algorithms for optimal motion planning,” *The international journal of robotics research*, vol. 30, no. 7, pp. 846–894, 2011.
- [4] Ahmed H Qureshi, Anthony Simeonov, Mayur J Bency, and Michael C Yip, “Motion planning networks,” in *2019 International Conference on Robotics and Automation (ICRA)*. IEEE, 2019, pp. 2118–2124.
- [5] Aviv Tamar, Yi Wu, Garrett Thomas, Sergey Levine, and Pieter Abbeel, “Value iteration networks,” *Advances in neural information processing systems*, vol. 29, 2016.
- [6] Jonathan D Gammell, Siddhartha S Srinivasa, and Timothy D Barfoot, “Informed rrt*: Optimal sampling-based path planning focused via direct sampling of an admissible ellipsoidal heuristic,” in *2014 IEEE/RSJ International Conference on Intelligent Robots and Systems*. IEEE, 2014, pp. 2997–3004.
- [7] Jonathan D Gammell, Siddhartha S Srinivasa, and Timothy D Barfoot, “Batch informed trees (bit): Sampling-based optimal planning via the heuristically guided search of implicit random geometric graphs,” in *2015 IEEE international conference on robotics and automation (ICRA)*. IEEE, 2015, pp. 3067–3074.
- [8] Jiankun Wang, Wenzheng Chi, Chenming Li, Chaoqun Wang, and Max Q-H Meng, “Neural rrt*: Learning-based optimal path planning,” *IEEE Transactions on Automation Science and Engineering*, vol. 17, no. 4, pp. 1748–1758, 2020.
- [9] Tingguang Chen, Tingxiang Huang, Xiao Xu, Gilbert Laporte, and Yang Liu, “Motion planning networks,” in *Proceedings of the IEEE/CVF Conference on Computer Vision and Pattern Recognition*, 2019, pp. 8537–8546.
- [10] Xinyu Xie and Danyang Yang, “Neural informed rrt*: A learning-based approach to motion planning,” in *2019 International Conference on Robotics and Automation (ICRA)*. IEEE, 2019, pp. 2845–2851.
- [11] Tsung-Yi Lin, Priya Goyal, Ross Girshick, Kaiming He, and Piotr Dollár, “Focal loss for dense object detection,” in *Proceedings of the IEEE international conference on computer vision*, 2017, pp. 2980–2988.
- [12] Olaf Ronneberger, Philipp Fischer, and Thomas Brox, “U-net: Convolutional networks for biomedical image segmentation,” in *International Conference on Medical image computing and computer-assisted intervention*. Springer, 2015, pp. 234–241.
- [13] Kaiming He, Xiangyu Zhang, Shaoqing Ren, and Jian Sun, “Deep residual learning for image recognition,” in *Proceedings of the IEEE conference on computer vision and pattern recognition*, 2016, pp. 770–778.